| | |
|---|---|
| Title | Three-dimensional vibration analysis of prisms with isosceles triangular cross-section |
| Author(s) | Zhou, D; Cheung, YK; Lo, SH; Au, FTK |
| Citation | Archive Of Applied Mechanics, 2010, v. 80 n. 6, p. 699-710 |
| Issued Date | 2010 |
| URL | http://hdl.handle.net/10722/124008 |
| Rights | Creative Commons: Attribution 3.0 Hong Kong License |

Arch Appl Mech (2010) 80: 699–710
DOI 10.1007/s00419-009-0337-7

ORIGINAL

**Ding Zhou · Y. K. Cheung · S. H. Lo · F. T. K. Au**

# Three-dimensional vibration analysis of prisms with isosceles triangular cross-section

Received: 8 September 2008 / Accepted: 28 May 2009 / Published online: 16 June 2009


**Abstract** This paper studies the three-dimensional (3-D) free vibration of uniform prisms with isosceles triangular cross-section, based on the exact, linear and small strain elasticity theory. The actual triangular prismatic domain is first mapped onto a basic cubic domain. Then the Ritz method is applied to derive the eigenfrequency equation from the energy functional of the prism. A set of triplicate Chebyshev polynomial series, multiplied by a boundary function chosen to, a priori, satisfy the geometric boundary conditions of the prism is developed as the admissible functions of each displacement component. The convergence and comparison study demonstrates the high accuracy and numerical robustness of the present method. The effect of length-thickness ratio and apex angle on eigenfrequencies of the prisms is studied in detail and the results are compared with those obtained from the classical one-dimensional theory and the 3-D finite element method. Sets of valuable data known for the first time are reported, which can serve as benchmark values in applying various approximate beam and rod theories.

**Keywords** Three-dimensional vibration · Elasticity solution · Prism · Triangular cross-section · Ritz method

## 1 Introduction

Uniform prisms with isosceles triangular cross-section can be found as basic structural elements in civil, mechanical and bridge engineering. In many cases, they have to bear the dynamic loads, and therefore, to understand their dynamic characteristics is very important for the safety and reliability of structures.

Various one-dimensional (1-D) models to describe the elastic deformation in a prism have been developed, in which Euler–Bernoulli beam theory [1] and Timoshenko beam theory [2] are two of the most famous ones. In the 1-D approximate theories, vibration modes of a prism can be divided into three distinct categories: longitudinal vibration [3], torsional vibration [4] and flexural vibration [1,2,5], respectively, through considering the prisms as slender beams or rods. In general, the longitudinal vibration of a prism can be individually modeled, and the torsional vibration and the flexural vibration is dependent of the locations of elastic axis and inertial axis of the prism. When the elastic axis is coincident with the inertial axis, the torsional vibration and the flexural vibration is uncoupled, otherwise coupling will occur.

Owing to some severe assumptions imposed on the deformations in a prism, the accuracy of the 1-D approximate theories greatly depends on the length-thickness ratio of the prism, and its applicability is also dependent of what accuracy would be required for the actual situation. Therefore, the accuracy of 1-D theories should be checked by the solutions from the exact three-dimensional (3-D) elasticity theory where no

D. Zhou (✉)
College of Civil Engineering, Nanjing University of Technology, 210009 Nanjing, People's Republic of China
E-mail: dingzhou57@yahoo.com

Y. K. Cheung · S. H. Lo · F. T. K. Au
Department of Civil Engineering, The University of Hong Kong, Hong Kong, People's Republic of China

artificial, kinematic constraints are placed on the deformations. A close scrutiny among the references reveals that study on 3-D vibration of prisms has received little attention because of the difficulty of attaining accurate solutions. The available references mainly focused on the prisms with circular or rectangular cross-section. Hutchinson [6,7] studied the vibration of a completely free prism with circular cross-section and compared his 3-D solutions with the approximate 1-D solutions [8]. Such a prism was also studied by Leissa and So [9] using the Ritz method for the free-free and the fixed-free end conditions. Fromme and Leissa [10] used the so-called Fourier associated-periodicity extension method to study the 3-D vibration of a completely free prism with rectangular cross-section. The same problem was also studied by Hutchinson and Zillmer [11] using the method of series solution. Furthermore, Leissa and Zhang [12] used the Ritz method to study the 3-D vibration of a cantilevered prism with rectangular cross-section, while Leissa and Jacob [13] and McGree [14], respectively, used the Ritz method to study the 3-D vibration of a cantilevered twisted prism with rectangular cross-section. Recently, Liew et al. [15] used the Ritz method to study the 3-D free vibration of prisms with the thick-walled, open sections of L, T, C and I shapes. Lim [16] investigated the effect of hypothetical assumption of neglecting flexural normal stress in vibration analysis for a cantilevered prism with rectangular cross-section. Up to now, most of the research work on 3-D vibration analysis of structural components is performed by the Ritz method because of its simplicity in analysis [9,12–16], in which two types of polynomial functions are commonly used as the basis of admissible functions: the simple algebraic polynomials [9,12–14,16] and the orthogonal polynomials [15]. It is well known that the simple algebraic polynomials have the straightforward and convenient characteristics in programming and computing. However, undesirable ill-conditioning occurs generally so early that only a small part of the lower-order eigenfrequencies can be obtained with satisfactory results. Especially, for a prism with noncircular or nonrectangular cross-section, the applicability of the simple algebraic polynomials is greatly reduced, as demonstrated by the authors in a recent paper on vibration analysis of cantilevered skew thick plates [17]. The ill-conditioning situation can be improved by employing the orthogonal polynomials instead of the natural ones. However, as So and Leissa [18] pointed out, this would not only complicate the analysis but may yield inaccurate results due to the truncation errors which arise in calculating orthogonal polynomials by the Gram-Schmidt process. In this paper, the Chebyshev polynomials are suggested as the alternative basic functions to study the prisms with isosceles triangular cross-section using the Ritz method. Not only high accuracy and numerical robustness can be obtained due to the excellent properties of the Chebyshev polynomials in function approximation [19], but also simplicity in programming and computing can be maintained because of the Chebyshev polynomials can be conveniently expressed as cosine functions.

## 2 Formulation

Consider a prism with isosceles triangular cross-section of width $a$, length $h$ and apex angle $\alpha$ as shown in Fig. 1a. Based on the exact, linear and small-strain 3-D elasticity theory, the strain energy $\overline{V}$ and the kinetic

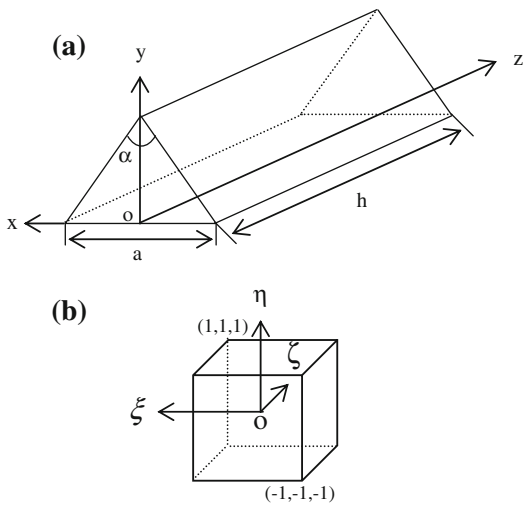


**Fig. 1** A prism with isosceles triangular cross-section: **a** sketch, coordinates and sizes; **b** domain transformation into a basic cube

energy $\overline{T}$ of an elastic body undergoing free vibration are given by the volume integrals

$$\begin{aligned}\overline{V} &= (1/2)\iiint [\lambda(\varepsilon_x+\varepsilon_y+\varepsilon_z)^2 + 2G(\varepsilon_x^2+\varepsilon_y^2+\varepsilon_z^2) + G(\gamma_{xy}^2+\gamma_{yz}^2+\gamma_{zx}^2)]\mathrm{d}x\mathrm{d}y\mathrm{d}z,\\ \overline{T} &= (\rho/2)\iiint (\dot{u}^2+\dot{v}^2+\dot{w}^2)\mathrm{d}x\mathrm{d}y\mathrm{d}z,\end{aligned} \tag{1}$$

where $\rho$ is the mass per unit volume; $u = u(x, y, z)$, $v = v(x, y, z)$ and $w = w(x, y, z)$ are displacement components at a generic point in the $x$, $y$ and $z$ directions, respectively; $\dot{u}$, $\dot{v}$ and $\dot{w}$ are the corresponding velocity components. $\lambda$ and $G$ are the Lamè constants for a homogeneous and isotropic material. $\varepsilon_i$ and $\gamma_{ij}(i, j = x, y, z)$ are the strain components.

For free vibrations, the displacement components of the 3-D elastic body may be expressed as

$$u = U(x, y, z)\mathrm{e}^{i\omega t}, \quad v = V(x, y, z)\mathrm{e}^{i\omega t}, \quad w = W(x, y, z)\mathrm{e}^{i\omega t}, \tag{2}$$

where $\omega$ is the circular eigenfrequency of vibration.

Substituting Eq. (2) into Eq. (1), the maximum strain energy $\overline{V}_{\max}$ and the maximum kinetic energy $\overline{T}_{\max}$ of the prism are, respectively, expressed as

$$\begin{aligned}\overline{V}_{\max} &= (1/2)\iiint \left[\lambda\overline{V}_1 + G(\overline{V}_2+\overline{V}_3)\right]\mathrm{d}x\mathrm{d}y\mathrm{d}z,\\ \overline{T}_{\max} &= (1/2)\rho\omega^2\iiint (U^2+V^2+W^2)\mathrm{d}x\mathrm{d}y\mathrm{d}z,\end{aligned} \tag{3}$$

in which,

$$\begin{aligned}\overline{V}_1 &= (\partial U/\partial x + \partial V/\partial y + \partial W/\partial z)^2,\\ \overline{V}_2 &= 2(\partial U/\partial x)^2 + 2(\partial V/\partial y)^2 + 2(\partial W/\partial z)^2,\\ \overline{V}_3 &= (\partial U/\partial y + \partial V/\partial x)^2 + (\partial V/\partial z + \partial W/\partial y)^2 + (\partial W/\partial x + \partial U/\partial z)^2.\end{aligned} \tag{4}$$

The Lagrangian energy functional $\Re$ is given as

$$\Re = \overline{T}_{\max} - \overline{V}_{\max}. \tag{5}$$

For simplicity in constructing admissible functions, the actual triangular prismatic domain is mapped onto a basic cubic domain, as shown in Fig. 1b, using the following co-ordinate transformation

$$x = a\xi(1-\eta)/4, \quad y = a(1+\cos\alpha)(1+\eta)/(4\sin\alpha), \quad z = h(\zeta+1)/2. \tag{6}$$

Applying the chain rule of differentiation, the relation of the first derivative between the original co-ordinate system $x - y - z$ and the new co-ordinate system $\xi - \eta - \zeta$ can be expressed as

$$\begin{Bmatrix} \dfrac{\partial()}{\partial x} \\ \dfrac{\partial()}{\partial y} \\ \dfrac{\partial()}{\partial z} \end{Bmatrix} = J^{-1} \begin{Bmatrix} \dfrac{\partial()}{\partial \xi} \\ \dfrac{\partial()}{\partial \eta} \\ \dfrac{\partial()}{\partial \zeta} \end{Bmatrix}, \tag{7}$$

where $\boldsymbol{J}$ denotes the Jacobian matrix of the geometrical mapping as follows

$$J = \begin{bmatrix} \dfrac{\partial x}{\partial \xi} & \dfrac{\partial y}{\partial \xi} & \dfrac{\partial z}{\partial \xi} \\ \dfrac{\partial x}{\partial \eta} & \dfrac{\partial y}{\partial \eta} & \dfrac{\partial z}{\partial \eta} \\ \dfrac{\partial x}{\partial \zeta} & \dfrac{\partial y}{\partial \zeta} & \dfrac{\partial z}{\partial \zeta} \end{bmatrix} = \begin{bmatrix} (1-\eta)a/4 & 0 & 0 \\ -\xi a/4 & (1+\cos\alpha)a/(4\sin\alpha) & 0 \\ 0 & 0 & h/2 \end{bmatrix}. \tag{8}$$

Equations (7) and (8) will be used later to transform the $x-y-z$ domain integrals in Eq. (3) into the $\xi-\eta-\zeta$ domain integrals.

Following the above co-ordinate transformation, the displacement functions $U(x,y,z)=U(\xi,\eta,\zeta)$, $V(x,y,z)=V(\xi,\eta,\zeta)$ and $W(x,y,z)=W(\xi,\eta,\zeta)$ are approximately expressed in terms of a finite series as

$$\begin{aligned} U(\xi,\eta,\zeta) &= f_u(\zeta)\sum_{i=1}^{I}\sum_{j=1}^{J}\sum_{k=1}^{K}A_{ijk}F_i(\xi)F_j(\eta)F_k(\zeta),\\ V(\xi,\eta,\zeta) &= f_v(\zeta)\sum_{l=1}^{L}\sum_{m=1}^{M}\sum_{n=1}^{N}B_{lmn}F_l(\xi)F_m(\eta)F_n(\zeta),\\ W(\xi,\eta,\zeta) &= f_w(\zeta)\sum_{p=1}^{P}\sum_{q=1}^{Q}\sum_{r=1}^{R}C_{pqr}F_p(\xi)F_q(\eta)F_r(\zeta), \end{aligned} \tag{9}$$

where $A_{ijk}$, $B_{lmn}$ and $C_{pqr}$ are undetermined coefficients, $f_u(\zeta)$, $f_v(\zeta)$ and $f_w(\zeta)$ are the boundary functions while all the series functions have an identical form of formulation: $F_s(\chi)(s=i,j,k,l,m,n,p,q,r$ and $\chi=\xi,\eta,\zeta)$ which are a set of Chebyshev polynomials [19] defined in interval $[-1,1]$, and is expressed by

$$F_s(\chi)=\cos[(s-1)\arccos(\chi)],\quad s=1,2,3,\ldots \tag{10}$$

It should be noted that Chebyshev polynomial functions $F_s(\chi)(s=1,2,3,\ldots)$ is a set of complete and orthogonal series in the interval $[-1,1]$. This ensures that the triplicate series $F_i(\xi)F_j(\eta)F_k(\zeta)(i,j,k=1,2,3,\ldots)$ is also a complete and orthogonal set in the cubic domain. Compared to results using other polynomial series such as the Taylor series, more rapid convergence and robustness in numerical computation can be expected. Moreover, the Chebyshev polynomials can be expressed in terms of cosine functions, which provides a convenient way in programming.

In the Ritz method, the stress boundary conditions of the plates need not be satisfied in advance. However, the geometric boundary conditions should be satisfied exactly. For a prism, the boundary functions in the admissible functions should only relate with the $\zeta$ coordinate but not the $\xi$ and $\eta$ coordinates because there are no displacement constraints on the lateral surface of the prism. Some common boundary functions are shown in Table 1.

Substituting Eqs. (6–8) into Eqs. (3–5), the Lagrangian functional $\Re$ can be expressed in terms of the co-ordinate system $\xi-\eta-\zeta$. Then substituting Eq. (9) into the functional expression, and upon minimizing $\Re$ with respect to the undetermined coefficients $A_{ijk}$, $B_{lmn}$ and $C_{pqr}$, a set of eigenfrequency equations is derived, which can be written in matrix form as

$$\left(\begin{bmatrix} [K_{uu}] & [K_{uv}] & [K_{uw}]\\ [K_{uv}]^T & [K_{vv}] & [K_{vw}]\\ [K_{uw}]^T & [K_{vw}]^T & [K_{ww}] \end{bmatrix} - \Omega^2 \begin{bmatrix} [M_{uu}] & 0 & 0\\ 0 & [M_{vv}] & 0\\ 0 & 0 & [M_{ww}] \end{bmatrix}\right) \begin{Bmatrix} \{A\}\\ \{B\}\\ \{C\} \end{Bmatrix} = \begin{Bmatrix} \{0\}\\ \{0\}\\ \{0\} \end{Bmatrix}, \tag{11}$$

**Table 1** The boundary functions corresponding to common boundary conditions

| B.C. | $f_u(\zeta)$ | $f_v(\zeta)$ | $f_w(\zeta)$ |
|---|---|---|---|
| F-F | 1 | 1 | 1 |
| C-F | $1+\zeta$ | $1+\zeta$ | $1+\zeta$ |
| C-S | $1-\zeta^2$ | $1-\zeta^2$ | $1+\zeta$ |
| C-C | $1-\zeta^2$ | $1-\zeta^2$ | $1-\zeta^2$ |
| S-F | $1+\zeta$ | $1+\zeta$ | 1 |
| S-S | $1-\zeta^2$ | $1-\zeta^2$ | 1 |

F, C and S mean free, clamped and simply-supported ends, respectively, and the first capital means the boundary condition at $z=0$ and the second one means that at $z=h$
*B.C.* boundary conditions

in which $\Omega = \omega h\sqrt{\rho/E}$ . $[K_{ij}]$ and $[M_{ii}]$ $(i, j = u, v, w)$ are the stiffness sub-matrices and the diagonal mass sub-matrices and $\{A\}$, $\{B\}$ and $\{C\}$ are the column vectors of unknown coefficients, which are given as follows

$$\{A\} = \begin{Bmatrix} A_{111} \\ A_{112} \\ \vdots \\ A_{11K} \\ A_{121} \\ \vdots \\ A_{12K} \\ \vdots \\ A_{1JK} \\ \vdots \\ A_{IJK} \end{Bmatrix}, \quad \{B\} = \begin{Bmatrix} B_{111} \\ B_{112} \\ \vdots \\ B_{11N} \\ B_{121} \\ \vdots \\ B_{12N} \\ \vdots \\ B_{1MN} \\ \vdots \\ B_{LMN} \end{Bmatrix}, \quad \{C\} = \begin{Bmatrix} C_{111} \\ C_{112} \\ \vdots \\ C_{11R} \\ C_{121} \\ \vdots \\ C_{12R} \\ \vdots \\ C_{1QR} \\ \vdots \\ C_{PQR} \end{Bmatrix}. \tag{12}$$

Various elements in sub-matrices $[K_{ij}]$ and $[M_{ii}](i, j = u, v, w)$ are given by

$$\begin{aligned}
[K_{uu}] &= \frac{(1-\nu)(1+\cos\alpha)}{(1-2\nu)\sin\alpha} E^{110}_{uiu\bar{i}} G^{00-1}_{uju\bar{j}} H^{00}_{uku\bar{k}} + \frac{\sin\alpha}{2(1+\cos\alpha)} (E^{112}_{uiu\bar{i}} G^{00-1}_{uju\bar{j}} + E^{00}_{uiu\bar{i}} G^{111}_{uju\bar{j}} \\
&\quad + E^{101}_{uiu\bar{i}} G^{010}_{uju\bar{j}} + E^{011}_{uiu\bar{i}} G^{100}_{uju\bar{j}}) H^{00}_{uku\bar{k}} + \frac{1+\cos\alpha}{8\gamma^2\sin\alpha} E^{000}_{uiu\bar{i}} G^{001}_{uju\bar{j}} H^{00}_{uku\bar{k}}, \\
[K_{vv}] &= \frac{(1-\nu)\sin\alpha}{(1-2\nu)(1+\cos\alpha)} (E^{112}_{vlv\bar{l}} G^{00-1}_{vmv\bar{m}} + E^{000}_{vlv\bar{l}} G^{111}_{vmv\bar{m}} + E^{101}_{vlv\bar{l}} G^{010}_{vmv\bar{m}} + E^{011}_{vlv\bar{l}} G^{100}_{vmv\bar{m}}) H^{00}_{vnv\bar{n}} \\
&\quad + \frac{1+\cos\alpha}{8\gamma^2\sin\alpha} E^{000}_{vlv\bar{l}} G^{001}_{vmv\bar{m}} H^{11}_{vnv\bar{n}} + \frac{1+\cos\alpha}{2\sin\alpha} E^{110}_{vlv\bar{l}} G^{00-1}_{vmv\bar{m}} H^{00}_{vnv\bar{n}}, \\
[K_{ww}] &= \frac{(1-\nu)(1+\cos\alpha)}{4(1-2\nu)\gamma^2\sin\alpha} E^{000}_{wpw\bar{p}} G^{001}_{wqw\bar{q}} H^{11}_{wrw\bar{r}} + \frac{\sin\alpha}{2(1+\cos\alpha)} (E^{112}_{wpw\bar{p}} G^{00-1}_{wqw\bar{q}} + E^{000}_{wpw\bar{p}} G^{111}_{wqw\bar{q}} \\
&\quad + E^{101}_{wpw\bar{p}} G^{010}_{wqw\bar{q}} + E^{011}_{wpw\bar{p}} G^{100}_{wqw\bar{q}}) H^{00}_{wrw\bar{r}} + \frac{1+\cos\alpha}{2\sin\alpha} E^{110}_{wpw\bar{p}} G^{00-1}_{wqw\bar{q}} H^{00}_{wrw\bar{r}}, \\
[K_{uv}] &= \frac{\nu}{1-2\nu} (E^{111}_{uiv\bar{l}} G^{00-1}_{ujv\bar{m}} + E^{100}_{uiv\bar{l}} G^{010}_{ujv\bar{m}}) H^{00}_{ukv\bar{n}} + \frac{1}{2} (E^{111}_{uiv\bar{l}} G^{00-1}_{ujv\bar{m}} + E^{010}_{uiv\bar{l}} G^{100}_{ujv\bar{m}}) H^{00}_{ukv\bar{n}}, \\
[K_{uw}] &= \frac{(1+\cos\alpha)}{4\gamma\sin\alpha} \left( \frac{2\nu}{1-2\nu} E^{100}_{uiw\bar{p}} G^{000}_{ujw\bar{q}} H^{01}_{ukw\bar{r}} + E^{010}_{uiw\bar{p}} G^{000}_{ujw\bar{q}} H^{10}_{ukw\bar{r}} \right), \\
[K_{vw}] &= \frac{1}{4\gamma} \left[ \frac{2\nu}{1-2\nu} (E^{101}_{vlw\bar{p}} G^{000}_{vmw\bar{q}} + E^{000}_{vlw\bar{p}} G^{101}_{vmw\bar{q}}) H^{01}_{vnw\bar{r}} \right. \\
&\quad \left. + (E^{011}_{vlw\bar{p}} G^{000}_{vmw\bar{q}} + E^{000}_{vlw\bar{p}} G^{011}_{vmw\bar{q}}) H^{10}_{vnw\bar{r}} \right], \\
[M_{uu}] &= \frac{(1+\nu)(1+\cos\alpha)}{16\gamma^2\sin\alpha} E^{000}_{uiu\bar{i}} G^{001}_{uju\bar{j}} H^{00}_{uku\bar{k}}, \\
[M_{vv}] &= \frac{(1+\nu)(1+\cos\alpha)}{16\gamma^2\sin\alpha} E^{000}_{vlv\bar{l}} G^{001}_{vmv\bar{m}} H^{00}_{vnv\bar{n}}, \\
[M_{ww}] &= \frac{(1+\nu)(1+\cos\alpha)}{16\gamma^2\sin\alpha} E^{000}_{wpw\bar{p}} G^{001}_{wqw\bar{q}} H^{00}_{wrw\bar{r}},
\end{aligned} \tag{13}$$

where

$$\gamma = h/a, \quad E^{\theta\sigma\varsigma}_{\alpha s\beta\bar{s}} = \int_{-1}^{1} \frac{\mathrm{d}^\theta F_s(\xi)}{\mathrm{d}\xi^\theta} \frac{\mathrm{d}^\sigma F_{\bar{s}}(\xi)}{\mathrm{d}\xi^\sigma} \xi^\varsigma \mathrm{d}\xi,$$

$$G^{\theta\sigma\tau}_{\alpha s\beta\bar{s}} = \int_{-1}^{1} \frac{\mathrm{d}^\theta F_s(\eta)}{\mathrm{d}\eta^\theta} \frac{\mathrm{d}^\sigma F_{\bar{s}}(\eta)}{\mathrm{d}\eta^\sigma} (1-\eta)^\tau \mathrm{d}\eta, \tag{14}$$

$$H^{\theta\sigma}_{\alpha s\beta\bar{s}} = \int_{-1}^{1} \frac{\mathrm{d}^\theta [f_\alpha(\zeta) F_s(\zeta)]}{\mathrm{d}\zeta^\theta} \frac{\mathrm{d}^\sigma [f_\beta(\zeta) F_{\bar{s}}(\zeta)]}{\mathrm{d}\zeta^\sigma} \mathrm{d}\zeta,$$

in which,

$$\begin{aligned} &\theta, \sigma = 0, 1, \quad \varsigma = 0, 1, 2, \quad \tau = -1, 0, 1, \quad \alpha, \beta = u, v, w, \\ &s = i, j, k, l, m, n, p, q, r, \quad \bar{s} = \bar{i}, \bar{j}, \bar{k}, \bar{l}, \bar{m}, \bar{n}, \bar{p}, \bar{q}, \bar{r}. \end{aligned} \tag{15}$$

It should be mentioned that the equations of the algebraic system (11) and its elements in (13), respectively, have been divided by the parameter $Ea^2/h$. A nontrivial solution is obtained by setting the determinant of the coefficient matrix of Eq. (11) equal to zero. Roots of the determinant are the square of the eigenvalues or nondimensional eigenfrequencies. Eigenfunctions, i.e. mode shapes, are determined by back-substitution of the eigenvalues, one-by-one, in the usual manner. All computations are performed in double precision (16 significant figures) on a microcomputer. The integrals in Eq. (14) are numerically evaluated by the piecewise Gaussian quadrature with 24 points.

## 3 Convergence and comparison study

It is obvious that for a prism with isosceles triangular cross-section, the 3-D vibration modes can be divided into two distinct categories: antisymmetric and symmetric ones of the bisecting plane about the apex $\alpha$, i.e. those about the $y - z$ (or $\eta - \zeta$) plane. It is well known that the Ritz method results in the upper eigenfrequencies and the eigenfrequencies should monotonically decrease with increasing the number of terms of the admissible functions. Although solution of any accuracy can be provided theoretically by using sufficient terms of admissible functions, the significant figures and capacity of the computer will inevitably result in a limitation to the number of terms of the admissible functions. Therefore, the choice of admissible functions becomes the successful key in the Ritz method. Moreover, suitable admissible functions not only should provide high accuracy and rapid convergence, but also should avoid the premature occurrence of ill-conditioning in numerical computation, which is of considerable importance for the 3-D Ritz analysis because of triplicate series generally has to be used.

A convergence study has been conducted for a prism with isosceles triangular cross-section. The length-thickness ratio of the prism is $h/a = 5$. Two different apex angles: $\alpha = 60^\mathrm{o}$ and $\alpha = 120^\mathrm{o}$ and three different boundary conditions: clamped-clamped, clamped-free and free-free are considered. For simplicity, equal numbers of terms of the Chebyshev polynomials were used in each displacement functions. The eigenfrequency parameters with respect to four groups of different numbers of terms of admissible functions: $I \times J \times K = 5 \times 5 \times 10, 6 \times 6 \times 15, 7 \times 7 \times 20$ and $8 \times 8 \times 25$, respectively, are studied. Table 2 gives the first eight antisymmetric modes about the bisecting plane of apex angle and Table 3 gives the first eight symmetric ones. The data accurate to the third figure after decimal point are examined and those underlined are the converged values for the smallest number of terms in $5 \times 5 \times 10$, $6 \times 6 \times 15$, $7 \times 7 \times 20$ and $8 \times 8 \times 25$. From these two tables, it is shown that the fastest convergence is for the F-F prisms while the slowest convergence is for the C-C prisms. One reason for this is that the fixed ends cause large stress gradients near the corners and another reason is that for the F-F prisms, the admissible functions is a set of orthogonal and complete series while for the C-C prisms, the orthogonality of the admissible functions is destroyed by the multiplying boundary functions, which require more terms to represent with reasonable accuracy. However, the main properties of the Chebyshev polynomials are preserved in the present admissible functions because the boundary functions are always invariable in sign.

In order to demonstrate the advantage of the Chebyshev polynomials in numerical robustness over the simple algebraic polynomials, the convergence for a C-F prism with the apex angle $\alpha = 60°$ and the length-thickness ratio $h/a = 5$, using the simple algebraic polynomials as the admissible functions, are given in Table 4. It is seen that when $6 \times 6 \times 12$ terms of simple algebraic polynomials are used, the computation becomes ill-conditioned. However, one can see from Tables 2 and 3 that even using $8 \times 8 \times 25$ terms of Chebyshev polunomials, a stable computation still has been obtained.

**Table 2** Convergence of the first eight eigenfrequency parameters for a prism with isosceles triangular cross-section and length-thickness ratio $h/a = 5$: antisymmetric modes about the bisecting plane of apex angle

| $\alpha$ | B.C. | $I \times J \times K$ | $\Omega_1$ | $\Omega_2$ | $\Omega_3$ | $\Omega_4$ | $\Omega_5$ | $\Omega_6$ | $\Omega_7$ | $\Omega_8$ |
|---|---|---|---|---|---|---|---|---|---|---|
| 60° | F-F | 5 × 5 × 10 | 0.852 | 1.509 | 2.108 | 3.016 | 3.662 | 4.519 | 5.357 | 6.025 |
| | | 6 × 6 × 15 | 0.852 | 1.509 | 2.108 | 3.016 | 3.660 | 4.518 | 5.336 | 6.015 |
| | | 7 × 7 × 20 | 0.852 | 1.509 | 2.108 | 3.016 | 3.660 | 4.518 | 5.336 | 6.015 |
| | | 8 × 8 × 25 | 0.852 | 1.509 | 2.108 | 3.016 | 3.660 | 4.518 | 5.336 | 6.015 |
| | C-F | 5 × 5 × 10 | 0.142 | 0.761 | 0.814 | 2.037 | 2.283 | 3.518 | 3.802 | 5.144 |
| | | 6 × 6 × 15 | 0.142 | 0.760 | 0.813 | 2.035 | 2.280 | 3.515 | 3.798 | 5.135 |
| | | 7 × 7 × 20 | 0.142 | 0.760 | 0.813 | 2.034 | 2.280 | 3.515 | 3.798 | 5.134 |
| | | 8 × 8 × 25 | 0.142 | 0.760 | 0.813 | 2.034 | 2.280 | 3.514 | 3.797 | 5.134 |
| | C-C | 5 × 5 × 10 | 0.812 | 1.535 | 1.964 | 3.068 | 3.386 | 4.601 | 4.948 | 6.129 |
| | | 6 × 6 × 15 | 0.810 | 1.533 | 1.961 | 3.064 | 3.382 | 4.593 | 4.943 | 6.119 |
| | | 7 × 7 × 20 | 0.810 | 1.532 | 1.960 | 3.063 | 3.381 | 4.592 | 4.942 | 6.117 |
| | | 8 × 8 × 25 | 0.810 | 1.532 | 1.960 | 3.063 | 3.380 | 4.592 | 4.941 | 6.116 |
| 120° | F-F | 5 × 5 × 10 | 0.854 | 0.961 | 1.924 | 2.118 | 2.906 | 3.540 | 4.070 | 4.636 |
| | | 6 × 6 × 15 | 0.854 | 0.961 | 1.922 | 2.118 | 2.904 | 3.536 | 4.064 | 4.610 |
| | | 7 × 7 × 20 | 0.854 | 0.960 | 1.922 | 2.118 | 2.903 | 3.535 | 4.063 | 4.609 |
| | | 8 × 8 × 25 | 0.854 | 0.960 | 1.922 | 2.118 | 2.903 | 3.535 | 4.063 | 4.609 |
| | C-F | 5 × 5 × 10 | 0.142 | 0.488 | 0.821 | 1.465 | 2.046 | 2.477 | 3.265 | 3.783 |
| | | 6 × 6 × 15 | 0.142 | 0.488 | 0.819 | 1.463 | 2.044 | 2.473 | 3.260 | 3.778 |
| | | 7 × 7 × 20 | 0.142 | 0.487 | 0.819 | 1.462 | 2.043 | 2.472 | 3.259 | 3.776 |
| | | 8 × 8 × 25 | 0.142 | 0.487 | 0.819 | 1.462 | 2.043 | 2.471 | 3.259 | 3.776 |
| | C-C | 5 × 5 × 10 | 0.804 | 1.015 | 1.851 | 2.159 | 2.871 | 3.631 | 3.850 | 4.826 |
| | | 6 × 6 × 15 | 0.802 | 1.013 | 1.848 | 2.156 | 2.865 | 3.625 | 3.843 | 4.806 |
| | | 7 × 7 × 20 | 0.802 | 1.012 | 1.846 | 2.154 | 2.864 | 3.624 | 3.841 | 4.805 |
| | | 8 × 8 × 25 | 0.802 | 1.012 | 1.846 | 2.154 | 2.863 | 3.623 | 3.840 | 4.804 |

**Table 3** Convergence of the first eight eigenfrequency parameters for a prism with isosceles triangular cross-section and length-thickness ratio $h/a = 5$: symmetric modes about the bisecting plane of apex angle

| $\alpha$ | B.C. | $I \times J \times K$ | $\Omega_1$ | $\Omega_2$ | $\Omega_3$ | $\Omega_4$ | $\Omega_5$ | $\Omega_6$ | $\Omega_7$ | $\Omega_8$ |
|---|---|---|---|---|---|---|---|---|---|---|
| 60° | F-F | 5 × 5 × 10 | 0.852 | 2.108 | 3.137 | 3.662 | 5.357 | 6.244 | 7.483 | 9.281 |
| | | 6 × 6 × 15 | 0.852 | 2.108 | 3.137 | 3.660 | 5.336 | 6.244 | 7.048 | 8.743 |
| | | 7 × 7 × 20 | 0.852 | 2.108 | 3.137 | 3.660 | 5.336 | 6.244 | 7.048 | 8.735 |
| | | 8 × 8 × 25 | 0.852 | 2.108 | 3.137 | 3.660 | 5.336 | 6.244 | 7.048 | 8.735 |
| | C-F | 5 × 5 × 10 | 0.142 | 0.814 | 1.578 | 2.037 | 3.519 | 4.719 | 5.144 | 6.860 |
| | | 6 × 6 × 15 | 0.142 | 0.813 | 1.577 | 2.035 | 3.516 | 4.717 | 5.135 | 6.812 |
| | | 7 × 7 × 20 | 0.142 | 0.813 | 1.577 | 2.034 | 3.516 | 4.717 | 5.134 | 6.811 |
| | | 8 × 8 × 25 | 0.142 | 0.813 | 1.577 | 2.034 | 3.515 | 4.717 | 5.134 | 6.811 |
| | C-C | 5 × 5 × 10 | 0.812 | 1.964 | 3.166 | 3.387 | 4.950 | 6.306 | 6.603 | 8.336 |
| | | 6 × 6 × 15 | 0.810 | 1.961 | 3.164 | 3.382 | 4.944 | 6.302 | 6.583 | 8.255 |
| | | 7 × 7 × 20 | 0.810 | 1.960 | 3.164 | 3.381 | 4.942 | 6.300 | 6.581 | 8.253 |
| | | 8 × 8 × 25 | 0.810 | 1.960 | 3.164 | 3.381 | 4.942 | 6.300 | 6.580 | 8.252 |
| 120° | F-F | 5 × 5 × 10 | 0.301 | 0.809 | 1.531 | 2.432 | 3.139 | 3.861 | 5.547 | 6.261 |
| | | 6 × 6 × 15 | 0.301 | 0.809 | 1.530 | 2.418 | 3.139 | 3.430 | 4.535 | 5.685 |
| | | 7 × 7 × 20 | 0.301 | 0.809 | 1.530 | 2.418 | 3.319 | 3.430 | 4.527 | 5.671 |
| | | 8 × 8 × 25 | 0.301 | 0.809 | 1.530 | 2.418 | 3.319 | 3.430 | 4.527 | 5.671 |
| | C-F | 5 × 5 × 10 | 0.048 | 0.296 | 0.806 | 1.518 | 1.576 | 2.403 | 3.433 | 4.721 |
| | | 6 × 6 × 15 | 0.048 | 0.295 | 0.804 | 1.516 | 1.575 | 2.392 | 3.391 | 4.473 |
| | | 7 × 7 × 20 | 0.048 | 0.295 | 0.804 | 1.515 | 1.575 | 2.391 | 3.389 | 4.472 |
| | | 8 × 8 × 25 | 0.048 | 0.295 | 0.804 | 1.515 | 1.575 | 2.391 | 3.389 | 4.472 |
| | C-C | 5 × 5 × 10 | 0.301 | 0.801 | 1.506 | 2.372 | 3.161 | 3.381 | 4.515 | 6.306 |
| | | 6 × 6 × 15 | 0.300 | 0.799 | 1.502 | 2.367 | 3.158 | 3.350 | 4.421 | 5.540 |
| | | 7 × 7 × 20 | 0.300 | 0.798 | 1.501 | 2.365 | 3.157 | 3.349 | 4.418 | 5.538 |
| | | 8 × 8 × 25 | 0.299 | 0.798 | 1.501 | 2.364 | 3.157 | 3.348 | 4.417 | 5.536 |

**Table 4** Convergence of the first eight eigenfrequency parameters for a C-F prism with apex angle $\alpha = 60°$ and length-thickness ratio $h/a = 5$, using the simple algebraic polynomials as the admissible functions

| I×J×K | $\Omega_1$ | $\Omega_2$ | $\Omega_3$ | $\Omega_4$ | $\Omega_5$ | $\Omega_6$ | $\Omega_7$ | $\Omega_8$ |
|---|---|---|---|---|---|---|---|---|
| Symmetric modes about the bisecting plane of apex angle | | | | | | | | |
| $2 \times 2 \times 4$ | 0.162 | 0.926 | 1.590 | 2.955 | 4.780 | 6.061 | 8.882 | 14.715 |
| $3 \times 3 \times 6$ | 0.143 | 0.823 | 1.581 | 2.084 | 3.741 | 4.729 | 7.436 | 7.835 |
| $4 \times 4 \times 8$ | 0.142 | 0.815 | 1.579 | 2.040 | 3.536 | 4.722 | 5.305 | 7.444 |
| $5 \times 5 \times 10$ | 0.142 | 0.814 | 1.578 | 2.037 | 3.519 | 4.719 | 5.144 | 6.860 |
| $6 \times 6 \times 12$ | Ill-conditioned | | | | | | | |
| Antisymmetric modes about the bisecting plane of apex angle | | | | | | | | |
| $2 \times 2 \times 4$ | 0.150 | 0.867 | 0.923 | 2.770 | 2.839 | 4.988 | 5.829 | 9.561 |
| $3 \times 3 \times 6$ | 0.143 | 0.818 | 0.866 | 2.066 | 2.595 | 3.695 | 4.330 | 6.223 |
| $4 \times 4 \times 8$ | 0.142 | 0.762 | 0.815 | 2.039 | 2.287 | 2.523 | 3.813 | 5.296 |
| $5 \times 5 \times 10$ | 0.142 | 0.761 | 0.814 | 2.037 | 2.283 | 2.518 | 3.802 | 5.144 |
| $6 \times 6 \times 12$ | Ill-conditioned | | | | | | | |

**Table 5** Comparison of the first eight eigenfrequency parameters for a slender prism with equilateral triangular cross-section ($\alpha = 60°$, $h/a = 20$) between the present 3-D elasticity solutions and the classical 1-D approximate theory solutions

| B.C. | Solution | $\Omega_1$ | $\Omega_2$ | $\Omega_3$ | $\Omega_4$ | $\Omega_5$ | $\Omega_6$ | $\Omega_7$ | $\Omega_8$ |
|---|---|---|---|---|---|---|---|---|---|
| C-C | 3-D | 0.227 | 0.618 | 1.193 | 1.515* | 1.934 | 2.827 | 3.030* | 3.148** |
| | 1-D | 0.228 | 0.626 | 1.234 | 1.509 | 2.040 | 3.047 | 3.018 | 3.142 |
| C-F | 3-D | 0.036 | 0.224 | 0.620 | 0.756* | 1.197 | 1.572** | 1.944 | 2.268* |
| | 1-D | 0.036 | 0.225 | 0.630 | 0.755 | 1.234 | 1.571 | 2.040 | 2.264 |
| C-S | 3-D | 0.157 | 0.503 | 1.036 | 1.512* | 1.572** | 1.742 | 2.604 | 3.024* |
| | 1-D | 0.157 | 0.510 | 1.064 | 1.509 | 1.571 | 1.819 | 2.776 | 3.018 |
| F-F | 3-D | 0.227 | 0.621 | 1.202 | 1.509* | 1.954 | 2.861 | 3.018* | 3.141** |
| | 1-D | 0.228 | 0.626 | 1.234 | 1.509 | 2.040 | 3.047 | 3.018 | 3.142 |
| S-F | 3-D | 0.157 | 0.504 | 0.755* | 1.040 | 1.750 | 2.264* | 2.619 | 3.141** |
| | 1-D | 0.157 | 0.510 | 0.755 | 1.064 | 1.819 | 2.264 | 2.776 | 3.141 |
| S-S | 3-D | 0.101 | 0.399 | 0.889 | 1.509* | 1.556 | 2.387 | 3.018* | 3.141** |
| | 1-D | 0.101 | 0.403 | 0.907 | 1.509 | 1.612 | 2.518 | 3.018 | 3.141 |

Data with one asterisk are the torsional modes while data with two asterisks are the longitudinal modes

**Table 6** Comparison of the present solutions with the finite element (FE) solutions for prisms with isosceles triangular cross section of apex angle $\alpha = 90°$

| $h/a$ | Solution | $\Omega_1$ | $\Omega_2$ | $\Omega_3$ | $\Omega_4$ | $\Omega_5$ | $\Omega_6$ | $\Omega_7$ | $\Omega_8$ |
|---|---|---|---|---|---|---|---|---|---|
| Cantilevered | | | | | | | | | |
| 1.5 | Present | 0.263* | 0.417 | 0.690 | 1.241* | 1.585* | 1.613 | 2.048 | 2.691* |
| | FE | 0.266 | 0.419 | 0.699 | 1.260 | 1.586 | 1.619 | 2.084 | 2.761 |
| 3.0 | Present | 0.137* | 0.231 | 0.678 | 0.780* | 1.187 | 1.579* | 1.937* | 2.029 |
| | FE | 0.138 | 0.232 | 0.686 | 0.789 | 1.193 | 1.579 | 1.964 | 2.055 |
| Clamped at two ends | | | | | | | | | |
| 1.5 | Present | 1.202* | 1.373 | 1.611 | 2.516* | 2.713 | 3.159 | 3.186* | 3.803* |
| | FE | 1.255 | 1.408 | 1.619 | 2.589 | 2.807 | 3.169 | 3.192 | 4.005 |
| 3.0 | Present | 0.777* | 1.142 | 1.404 | 1.866* | 2.481 | 2.852 | 3.169* | 3.193* |
| | FE | 0.789 | 1.156 | 1.426 | 1.917 | 2.518 | 2.898 | 3.174 | 3.286 |

Data with asterisk are those for the symmetric modes about the bisecting plane of apex angle

A comparison study between the present 3-D solutions and the classical 1-D theory solutions is given in Table 5 for a cantilevered prism with equilateral triangular cross-section. The length-thickness ratio of the prism is $h/a = 20$, which means the prism is a slender one. Six groups of common boundary conditions are considered. In all the following analysis, Poisson's ratio $\nu = 0.3$ is fixed and the zero eigenfrequencies are excluded from the results. It is obvious that for a prism with equilateral triangular cross-section, the elastic axis is coincident with the inertial axis. In such a case, 1-D beam theory considers that the torsional vibration and the flexural vibration are uncoupled. It is shown that in general for a slender prism, the low-order eigenfrequencies from the 1-D theory accord reasonably with those from the 3-D theory and in the three types of different modes, the longitudinal and torsional modes have the best accuracy and no clear error can be observed. While for the flexural modes, when the order of eigenfrequencies rises the errors from the 1-D theory increase accordingly. In all kinds of the boundary conditions, the worst 1-D results always come from the prism with C-C ends and

**Table 7** The first eight eigenfrequency parameters of antisymmetric and symmetric modes about the bisecting plane of apex angle for thick prisms with isosceles triangular cross-section, apex angle $\alpha = 60°$

| B.C. | $h/a$ | $\Omega_1$ | $\Omega_2$ | $\Omega_3$ | $\Omega_4$ | $\Omega_5$ | $\Omega_6$ | $\Omega_7$ | $\Omega_8$ |
|---|---|---|---|---|---|---|---|---|---|
| Antisymmetric modes | | | | | | | | | |
| C-C | 1 | 1.623 | 1.655 | 3.093 | 3.071 | 3.194 | 3.924 | 4.188 | 4.332 |
| | 2 | 1.387 | 1.567 | 2.827 | 3.124 | 4.464 | 4.664 | 5.584 | 5.807 |
| | 4 | 0.955 | 1.538 | 2.219 | 3.074 | 3.725 | 4.606 | 5.337 | 6.133 |
| C-F | 1 | 0.548 | 0.782 | 1.700 | 2.292 | 2.710 | 2.934 | 3.478 | 3.615 |
| | 2 | 0.331 | 0.769 | 1.444 | 2.298 | 3.093 | 3.804 | 4.551 | 5.276 |
| | 4 | 0.176 | 0.762 | 0.967 | 2.284 | 2.332 | 3.802 | 3.904 | 5.313 |
| F-F | 1 | 1.484 | 2.181 | 2.500 | 2.727 | 2.848 | 3.119 | 3.262 | 3.508 |
| | 2 | 1.505 | 1.676 | 2.989 | 3.266 | 4.433 | 4.772 | 5.162 | 5.431 |
| | 4 | 1.030 | 1.509 | 2.445 | 3.013 | 4.102 | 4.511 | 5.804 | 5.999 |
| S-S | 1 | 1.238 | 1.505 | 2.598 | 2.920 | 2.950 | 2.993 | 3.941 | 3.999 |
| | 2 | 0.841 | 1.508 | 2.477 | 3.010 | 4.202 | 4.503 | 5.196 | 5.539 |
| | 4 | 0.477 | 1.509 | 1.682 | 3.016 | 3.248 | 4.520 | 4.954 | 6.020 |
| Symmetric modes | | | | | | | | | |
| C-C | 1 | 1.656 | 3.071 | 3.093 | 3.201 | 3.924 | 4.188 | 4.332 | 4.721 |
| | 2 | 1.388 | 2.827 | 3.184 | 4.464 | 5.584 | 5.807 | 6.124 | 6.157 |
| | 4 | 0.955 | 2.219 | 3.168 | 3.725 | 5.337 | 6.293 | 6.998 | 8.655 |
| C-F | 1 | 0.548 | 1.592 | 1.700 | 2.710 | 2.934 | 3.478 | 3.588 | 3.615 |
| | 2 | 0.331 | 1.444 | 1.584 | 3.093 | 4.552 | 4.654 | 5.404 | 5.505 |
| | 4 | 0.176 | 0.967 | 1.578 | 2.332 | 3.905 | 4.713 | 5.569 | 7.234 |
| F-F | 1 | 2.181 | 2.500 | 2.727 | 2.969 | 3.119 | 3.262 | 3.445 | 3.508 |
| | 2 | 1.676 | 3.110 | 3.266 | 4.772 | 5.162 | 5.431 | 5.535 | 5.771 |
| | 4 | 1.030 | 2.445 | 3.134 | 4.102 | 5.804 | 6.219 | 7.467 | 8.964 |
| S-S | 1 | 1.238 | 2.598 | 2.950 | 2.969 | 3.429 | 3.763 | 3.999 | 4.112 |
| | 2 | 0.841 | 2.477 | 3.110 | 4.202 | 5.196 | 5.539 | 5.841 | 5.899 |
| | 4 | 0.477 | 1.682 | 3.134 | 3.248 | 4.954 | 6.219 | 6.690 | 8.407 |

the biggest error between the 3-D and 1-D theories occurs at the sixth eigenfrequency (2.827 vs. 3.047), which is about 7.8%.

In order to further demonstrate the accuracy and correctness of the present method, a comparison study of the present solutions with the 3-D finite element solutions is given in Table 6 for the prisms with isosceles triangular cross-section of apex angle $\alpha = 90°$. Two kinds of boundary conditions: clamped at two ends and cantilevered, and two different length-thickness ratios: $h/a = 1.5$ and $h/a = 3.0$, are considered. In the computation, the following parameters are taken: $a = 1.0$, $\rho = 1.0$ and $E = 1.0$, and $64 \times 30 = 1{,}920$ (64 is the element number in the cross-section while 30 is that along the length direction) Wedge6 elements for $h/a = 1.5$ and $64 \times 60 = 3{,}840$ for $h/a = 3.0$ in commercial program Strand7 were used. The first eight frequency parameters are given for comparison. It is observed that the present solutions are in agreement with the finite element solutions for all cases.

## 4 Numerical results

In Tables 7, 8 and 9, the first eight eigenfrequency parameters of antisymmetric and symmetric modes about the bisecting plane of the apex angle are given for thick prisms with isosceles triangular cross-section. Three different apex angles $\alpha = 60°, 90°, 120°$, three different length-thickness ratios $h/a = 1, 2, 4$ and four different boundary conditions C-C, C-F, F-F, S-S are considered. It is shown that the first eigenfrequencies monotonically decrease with the increase of length-thickness ratio for all cases except for the F-F beams. Moreover, it is seen that the C-C prisms always provide the highest eigenfrequencies (if concluding the zero eigenrequencies of F-F prisms) because of the severest boundary constraints. It should be mentioned that the 3-D vibration modes of a prism can be also divided into three distinct types: flexural modes, longitudinal modes and torsional modes, which correspond to the 1-D solutions as shown in Table 5. Observing the data given in Table 7, one can find that for prisms with equilateral triangular cross-section ($\alpha = 60°$), a part of eigenfrequencies of the antisymmetric modes are the same as those of the symmetric modes. This comes from the symmetry of the equilateral triangle, i.e. there are just the same three bisecting planes of angles. For each bisecting plane, the vibration modes should be the same, which only can be ensured when the eigenfrequencies of antisymmetric modes of the flexural vibration are the same as those of symmetric modes of the flexural vibration. Therefore,

**Table 8** The first eight eigenfrequency parameters of antisymmetric and symmetric modes about the bisecting plane of apex angle for thick prisms with isosceles triangular cross-section, apex angle $\alpha = 90°$

| B.C. | $h/a$ | $\Omega_1$ | $\Omega_2$ | $\Omega_3$ | $\Omega_4$ | $\Omega_5$ | $\Omega_6$ | $\Omega_7$ | $\Omega_8$ |
|---|---|---|---|---|---|---|---|---|---|
| Antisymmetric modes | | | | | | | | | |
| C-C | 1 | 1.427 | 1.734 | 2.768 | 3.258 | 3.868 | 4.052 | 4.422 | 4.713 |
| | 2 | 1.320 | 1.501 | 2.655 | 3.039 | 3.992 | 4.795 | 5.278 | 6.284 |
| | 4 | 0.957 | 1.378 | 2.224 | 2.775 | 3.677 | 4.239 | 5.105 | 5.847 |
| C-F | 1 | 0.547 | 0.704 | 1.726 | 2.030 | 3.124 | 3.414 | 3.599 | 4.062 |
| | 2 | 0.331 | 0.684 | 1.464 | 2.042 | 3.078 | 3.466 | 4.431 | 4.983 |
| | 4 | 0.176 | 0.675 | 0.975 | 2.017 | 2.367 | 3.365 | 3.953 | 4.744 |
| F-F | 1 | 1.297 | 2.223 | 2.560 | 2.919 | 3.410 | 3.510 | 3.823 | 4.354 |
| | 2 | 1.327 | 1.690 | 2.632 | 3.326 | 3.926 | 4.795 | 5.376 | 5.816 |
| | 4 | 1.033 | 1.333 | 2.468 | 2.660 | 3.985 | 4.150 | 5.325 | 5.826 |
| S-S | 1 | 1.210 | 1.401 | 2.517 | 2.755 | 3.273 | 3.754 | 3.859 | 4.249 |
| | 2 | 0.847 | 1.340 | 2.419 | 2.801 | 3.777 | 4.628 | 5.033 | 5.511 |
| | 4 | 0.479 | 1.336 | 1.693 | 2.681 | 3.257 | 4.067 | 4.839 | 5.603 |
| Symmetric modes | | | | | | | | | |
| C-C | 1 | 1.405 | 2.717 | 2.741 | 3.196 | 3.673 | 4.041 | 4.631 | 4.812 |
| | 2 | 1.028 | 2.283 | 3.178 | 3.704 | 4.947 | 5.116 | 5.404 | 6.139 |
| | 4 | 0.614 | 1.543 | 2.741 | 3.163 | 4.092 | 5.526 | 6.298 | 6.992 |
| C-F | 1 | 0.371 | 1.461 | 1.589 | 2.404 | 2.858 | 3.074 | 3.602 | 4.030 |
| | 2 | 0.202 | 1.050 | 1.582 | 2.419 | 3.857 | 4.671 | 4.762 | 5.025 |
| | 4 | 0.103 | 0.611 | 1.576 | 1.582 | 2.817 | 4.209 | 4.716 | 5.676 |
| F-F | 1 | 1.714 | 2.388 | 2.440 | 3.028 | 3.179 | 3.285 | 3.382 | 3.896 |
| | 2 | 1.139 | 2.549 | 3.120 | 4.013 | 4.746 | 4.787 | 5.221 | 5.470 |
| | 4 | 0.632 | 1.619 | 2.899 | 3.137 | 4.332 | 5.829 | 6.241 | 7.319 |
| S-S | 1 | 0.895 | 2.661 | 2.688 | 3.036 | 3.675 | 3.729 | 3.897 | 4.358 |
| | 2 | 0.536 | 1.886 | 3.120 | 3.279 | 4.770 | 4.924 | 5.433 | 5.983 |
| | 4 | 0.284 | 1.072 | 2.217 | 3.137 | 3.578 | 5.049 | 6.241 | 6.557 |

**Table 9** The first eight eigenfrequency parameters of antisymmetric and symmetric modes about the bisecting plane of apex angle for thick prisms with isosceles triangular cross-section, apex angle $\alpha = 120°$

| B.C. | $h/a$ | $\Omega_1$ | $\Omega_2$ | $\Omega_3$ | $\Omega_4$ | $\Omega_5$ | $\Omega_6$ | $\Omega_7$ | $\Omega_8$ |
|---|---|---|---|---|---|---|---|---|---|
| Antisymmetric modes | | | | | | | | | |
| C-C | 1 | 1.086 | 1.762 | 2.100 | 3.052 | 3.163 | 3.282 | 3.906 | 3.981 |
| | 2 | 1.010 | 1.475 | 2.010 | 2.990 | 3.030 | 3.946 | 4.838 | 4.888 |
| | 4 | 0.912 | 1.063 | 1.918 | 2.381 | 2.903 | 3.872 | 3.989 | 4.830 |
| C-F | 1 | 0.492 | 0.582 | 1.461 | 1.805 | 2.368 | 2.910 | 3.259 | 3.403 |
| | 2 | 0.330 | 0.502 | 1.395 | 1.586 | 2.397 | 3.276 | 3.365 | 4.228 |
| | 4 | 0.176 | 0.489 | 0.975 | 1.472 | 2.268 | 2.574 | 3.313 | 4.132 |
| F-F | 1 | 0.936 | 1.765 | 2.394 | 2.589 | 2.850 | 3.027 | 3.089 | 3.436 |
| | 2 | 0.956 | 1.658 | 1.950 | 2.733 | 3.536 | 3.620 | 4.489 | 5.306 |
| | 4 | 0.960 | 1.033 | 1.922 | 2.436 | 2.937 | 3.664 | 4.415 | 4.621 |
| S-S | 1 | 0.932 | 1.339 | 1.854 | 2.768 | 2.873 | 3.135 | 3.326 | 3.687 |
| | 2 | 0.829 | 0.995 | 1.864 | 2.678 | 2.792 | 3.708 | 4.622 | 4.658 |
| | 4 | 0.479 | 0.965 | 1.657 | 1.991 | 2.771 | 3.498 | 3.727 | 4.661 |
| Symmetric modes | | | | | | | | | |
| C-C | 1 | 1.050 | 2.092 | 2.138 | 3.036 | 3.056 | 3.191 | 3.981 | 4.404 |
| | 2 | 0.675 | 1.613 | 2.716 | 3.173 | 3.794 | 3.816 | 4.188 | 4.828 |
| | 4 | 0.370 | 0.970 | 1.792 | 2.770 | 3.160 | 3.849 | 4.979 | 6.117 |
| C-F | 1 | 0.230 | 1.076 | 1.586 | 1.844 | 2.182 | 2.412 | 3.170 | 3.361 |
| | 2 | 0.119 | 0.677 | 1.580 | 1.665 | 2.789 | 3.619 | 3.830 | 4.028 |
| | 4 | 0.060 | 0.366 | 0.981 | 1.576 | 1.817 | 2.813 | 3.908 | 4.715 |
| F-F | 1 | 1.181 | 1.820 | 1.885 | 2.493 | 2.504 | 3.045 | 3.395 | 3.486 |
| | 2 | 0.709 | 1.715 | 2.862 | 3.123 | 3.613 | 3.646 | 4.016 | 4.104 |
| | 4 | 0.374 | 0.991 | 1.842 | 2.856 | 3.137 | 3.968 | 5.123 | 6.247 |
| S-S | 1 | 0.578 | 1.704 | 2.057 | 2.744 | 2.819 | 3.045 | 3.687 | 4.140 |
| | 2 | 0.322 | 1.157 | 2.255 | 3.123 | 3.408 | 3.774 | 4.117 | 4.490 |
| | 4 | 0.166 | 0.644 | 1.382 | 2.313 | 3.137 | 3.375 | 4.510 | 5.669 |

from Table 7 one can conclude that all of the duplicate eigenfrequencies belong to the flexural vibration while all of the mono eigenfrequencies in symmetric modes belong to the longitudinal vibration and all of the mono eigenfrequencies in antisymmetric modes belong to the torsional vibration.

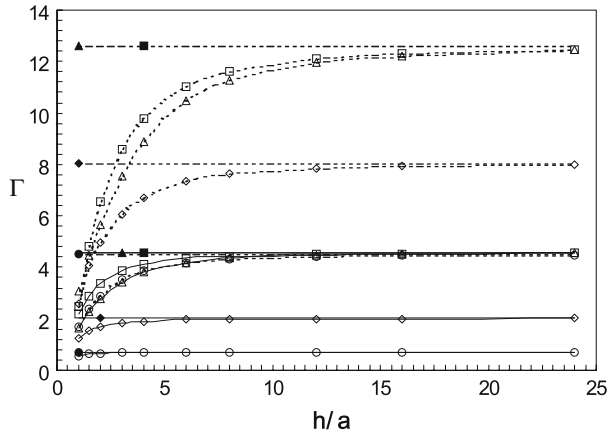


**Fig. 2** The first two modes of flexural vibration for prisms with equilateral triangular cross-section ($\alpha = 60°$), *dashed lines* the first modes; *dotted lines* the second modes, *open diamond* 3-D solutions of S-S prisms; *filled diamond* 1-D solutions of S-S prisms, *open triangle* 3-D solutions of F-F prisms; *filled triangle* 1-D solutions of F-F prisms, *open square* 3-D solutions of C-C prisms; *filled square* 1-D solutions of C-C prisms, *open circle* 3-D solutions of C-F prisms; *filled circle* 1-D solutions of C-F prisms

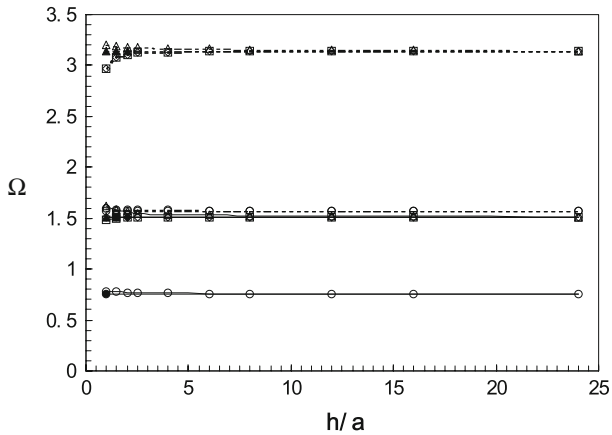


**Fig. 3** The fundamental modes of longitudinal and torsional vibrations for prisms with equilateral triangular cross-section ($\alpha = 60°$), *dashed lines* torsional; *dotted lines* longitudinal, *open diamond* 3-D solutions of S-S prisms; *filled diamond* 1-D solutions of S-S prisms, *open triangle* 3-D solutions of F-F prisms; *filled triangle* 1-D solutions of F-F prisms, *open square* 3-D solutions of C-C prisms; *filled square* 1-D solutions of C-C prisms, *open circle* 3-D solutions of C-F prisms; *filled circle* 1-D solutions of C-F prisms

Introducing a new dimensionless eigenfrequency parameter $\Gamma = (h/a)\Omega$ to describe the flexural vibration, the tendency of eigenfrequencies varying with increasing of the length-thickness ratio can be clearly shown. Again consider the prisms with equilateral triangular cross-section. Figure 2 gives the first two eigenfrequencies of flexural vibrations with respect to the length-thickness ratio, and Fig. 3 gives the fundamental eigenfrequencies of the longitudinal and torsional vibrations with respect to the length-thickness ratio. The varying interval of the length-thickness ratio $h/a$ is from 1 to 24. For convenience in comparison, the classical 1-D solutions are also given in the figures. It is shown that with the increase of length-thickness ratio, the 3-D solutions gradually become close to the 1-D solutions, however, the speed approaching to 1-D solutions decreases with the increasing eigenfrequency order. In these three different types of modes, the error of torsional vibration between the 3-D solutions and the 1-D solutions is the least and secondly the longitudinal vibration while the worst is the flexural vibration. It is seen that for the flexural vibration, the eigenfrequencies from the 1-D theory are always higher than those from the 3-D theory. Such an observation completely coincides with the basic assumption in the classical 1-D theory. However, this conclusion cannot be extended to the longitudinal vibration and the torsional vibration. Moreover, it is seen that for the flexural vibration, the 1-D solutions of the C-F prisms have the best accuracy while those of the C-C prisms have the worst accuracy.

## 5 Conclusion

In this paper, the 3-D vibration characteristics of uniform prisms with isosceles triangular cross-section are studied. The analysis process is based on the exact, linear and small strain elasticity and the Ritz method is applied to derive the eigenfrequency equation. Using a domain mapping, the integrals in a tri-prism domain are transferred into the integrals in a basic cubic domain. By selecting the Chebyshev polynomials which are multiplied by a boundary function to ensure the satisfaction of the geometric boundary conditions, the high accuracy and numerical robustness of the admissible functions are guaranteed. The convergence and comparison studies show the correctness of the present method. The effect of apex angle and length-thickness ratio on eigenfrequencies is investigated in detail and results known for the first time are reported.

## References

1. Clark, S.K.: Dynamics of Continuous Elements. Prentice-Hall, Englewood Cliffs (1972)
2. Timoshenko, S.P.: On the correction for shear of the differential equation for transverse vibrations of prismatic bars. Philos. Mag. **41**, 744–746 (1921)
3. Love, A.E.H.: A Treatise on the Mathematical Theory of Elasticity. Dover, New York (1944)
4. Rayleigh, J.W.S.: Theory of Sound. Dover, New York (1945)
5. Hutchinson, J.R.: Shear coefficients for Timoshenko beam theory. ASME J. Appl. Mech. **68**, 87–92 (2001)
6. Hutchinson, J.R.: Axisymmetric vibrations of a free finite length rod. J. Acoust. Soc. Am. **51**, 233–240 (1972)
7. Hutchinson, J.R.: Vibrations of solid cylinders. ASME J. Appl. Mech. **47**, 901–907 (1980)
8. Hutchinson, J.R.: Transverse vibrations of beams, exact versus approximate solutions. ASME J. Appl. Mech. **48**, 923–928 (1981)
9. Leissa, A.W., So, J.: Comparisons of vibration frequencies for rods and beams from 1-D and 3-D analysis. J. Acoust. Soc. Am. **98**, 2122–2135 (1991)
10. Fromme, A., Leissa, A.W.: Free vibration of the rectangular parallelepiped. J. Acoust. Soc. Am. **48**, 290–298 (1970)
11. Hutchinson, J.R., Zillimer, S.D.: Vibration of a free rectangular parallelepiped. ASME J. Appl. Mech. **50**, 123–130 (1983)
12. Leissa, A.W., Zhang, Z.D.: On the three-dimensional vibrations of the cantilevered rectangular parallelepiped. J. Acoust. Soc. Am. **73**, 2013–2021 (1983)
13. Leissa, A., Jacob, K.I.: Three-dimensional vibrations of twisted cantilevered parallelepipeds. ASME J. Appl. Mech. **53**, 614–618 (1986)
14. McGee, O.C.: Performance of continuum and discrete 3-diamendional vibration analysis of twisted cantilevered parallelepipeds. Comput. Struct. **42**, 211–227 (1992)
15. Liew, K.M., Hung, K.C., Lim, M.K.: Vibration of thick prismatic structures with three-dimensional flexibility. ASME J. Appl. Mech. **65**, 619–625 (1998)
16. Lim, C.W.: Three-dimensional vibration analysis of a cantilevered parallelepiped: Exact and approximate solutions. J. Acoust. Soc. Am. **106**, 3375–3381 (1999)
17. Zhou, D.: Three-dimensional vibration analysis of structural elements using chebyshev-ritz method. Ph.D. Thesis, Department of Civil Engineering, The University of Hong Kong (2003)
18. So, J., Leissa, A.W.: Free vibrations of thick hollow circular cylinders from three-dimensional analysis. J. Vib. Acoust. **119**, 89–95 (1997)
19. Fox, L., Parker, I.B.: Chebyshev Polynomials in Numerical Analysis. Oxford University Press, London (1968)